Characterization of the Successive One-Electron Oxidation Products of the Dicobalt Fulvalenediyl (Fv) Compound $Co_2Fv(CO)_4$ and its Phosphine-Substituted Product

Ayman Nafady† and William E. Geiger*

Department of Chemistry, University of Vermont, Burlington, Vermont 05405

Received June 11, 2008

The anodic oxidation of $Co_2Fv(CO)_4$, **1**, has been studied in dichloromethane containing $[NBu_4][TFAB]$ ($TFAB = [B(C_6F_5)_4]^-$) as the supporting electrolyte anion. Voltammetric, amperometric, coulometric, and *in situ* spectroelectrochemical methods showed that **1** is oxidized in two one-electron steps to $\mathbf{1}^+$ ($E_{1/2} = 0.06$ V) and $\mathbf{1}^{2+}$ ($E_{1/2} = 0.51$ V) in fast, diffusion-controlled processes without evidence of product adsorption at glassy carbon electrodes. Whereas the neutral compound has a *transoid* configuration of the two metals, IR and ESR spectra of the monocation $\mathbf{1}^+$ are best interpreted as arising from a *cisoid* structure with a Co−Co bond. Analysis of the ESR data suggests that the SOMO of $\mathbf{1}^+$ is significantly delocalized over the metal and ligand moieties. The discrete one-electron reactions of the $\mathbf{1/1}^+\mathbf{/1}^{2+}$ electron-transfer series stand in contrast to the direct two-electron processes observed for analogous group 6 and group 8 dileptic fulvalenediyl complexes. The radical cation $\mathbf{1}^+$ undergoes rapid substitution of a CO group when it is electrochemically generated in the presence of added PPh_3. Cyclic voltammetry simulations establish a substitution rate constant of 5×10^3 M^{-1} s^{-1} for the reaction. Bulk oxidation of **1** in the presence of 1 equiv of PPh_3 yields only the monosubstituted dication $[Co_2Fv(CO)_3(PPh_3)]^{2+}$, $\mathbf{2}^{2+}$, as shown by IR spectroscopy. One-electron back-reduction of $\mathbf{2}^{2+}$ to $\mathbf{2}^+$ allowed spectral identification of the radical cation of the substitution product. Study of the anodic products of $Co_2Fv(CO)_4$ was made possible by substitution of a traditional supporting electrolyte anion ($[PF_6]^-$ or $[BF_4]^-$) by the weakly coordinating TFAB anion.

Introduction

A number of studies have been published on the oxidation of fulvalenediyl (Fv, $C_{10}H_8$) complexes which are essentially composed of two 18-electron half-sandwich metal carbonyl compounds linked by the C−C bond of the bridging ligand.[1−5] Examples include metals of group 6 (e.g., ML = $[Cr(CO)_3]^-$),[2] group 7 (e.g., ML = $Mn(CO)_2PPh_3$),[3] and group 9 (e.g., ML = $Rh(CO)(PPh_3)$, $Rh(CO)_2$).[4,5] Cobalt dicarbonyl complexes are noticeably absent from this list and, among neutral dileptic[6] metal fulvalendiyl complexes, only $Rh_2Fv(CO)_4$ has been successfully oxidized in a chemically reversible process.[5] The

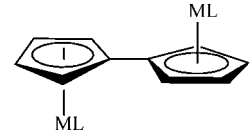

rather low ionization potential (7.26 eV) measured for the cobalt carbonyl complex $Co_2Fv(CO)_4$, ML = $Co(CO)_2$, **1**, by Lichtenberger et al.[7] suggests that this compound should, in fact, undergo facile oxidation. The finding that its two highest filled orbitals (HOMO and SHOMO) each bear a contribution from only one metal, and are separated by less than 0.3 eV,[7] implies that there is little electronic interaction between the two metal centers, in contrast to the behavior of the congeneric Rh system, which shows greater evidence of strong metal−metal orbital mixing.[7] Reasonably strong metal−metal interactions have also been observed in mixed-valent complexes derived from the oxidation of other fulvalenediyl half-sandwich type compounds, most notably those containing $Mn(CO)_2L'$ moieties (L′ = phosphine or phosphite).[3] To better understand the dicobalt system, we therefore set out to study the oxidation of **1**, keeping in mind that the increased lability of carbonyl ligands in metal carbonyl half-sandwich cation radicals[8] and the generally poor solubility of these charged species in lower-polarity solvents make the choice of the electrochemical medium (both solvent and supporting electrolyte) a critical factor if chemically reversible oxidations are to be observed. Electrolytes containing weakly coordinating anions[9] have been successfully used for the purpose of generating stable and soluble cations in low-

* Corresponding author. E-mail: william.geiger@uvm.edu.
† Present address: School of Chemistry, Monash University, Clayton, Victoria 3800, Australia.

(1) References for homodinuclear metal carbonyl complexes are given in refs 2−5. For heterodinuclear examples see: (a) Lacoste, M.; Delville-Desbois, M.-H.; Ardoin, N.; Astruc, D. *Organometallics* **1997**, *16*, 2343. (b) Brown, D.; Delville-Desbois, M.-H.; Vollhardt, K. P. C.; Astruc, D. *New J. Chem* **1992**, *16*, 899.

(2) (a) Moulton, R.; Weidman, T. W.; Vollhardt, P. C.; Bard, A. J. *Inorg. Chem.* **1986**, *25*, 1846. (b) Kovács, I.; Baird, M. C. *Organometallics* **1996**, *15*, 3588. (c) Kovács, I.; Baird, M. C. *Organometallics* **1996**, *15*, 4074. (d) Kovács, I.; Baird, M. C. *Organometallics* **1996**, *15*, 4084. (e) McGovern, P. A.; Vollhardt, K. P. C. *Chem. Commun.* **1996**, 1593.

(3) (a) Atwood, C. G.; Geiger, W. E. *J. Am. Chem. Soc.* **2000**, *122*, 5477. (b) Atwood, C. G.; Bitterwolf, T. E.; Geiger, W. E. *J. Electroanal. Chem.* **1995**, *397*, 279.

(4) (a) Connelly, N. G.; Lucy, A. R.; Payne, J. D.; Galas, A. M. R.; Geiger, W. E. *J. Chem. Soc., Dalton Trans.* **1983**, 1879. (b) Freeman, M. J.; Orpen, A. G.; Connelly, N. G.; Manners, I.; Raven, S. J. *J. Chem. Soc., Dalton Trans.* **1985**, 2283.

(5) Nafady, A.; Chin, T. T.; Geiger, W. E. *Organometallics* **2006**, *25*, 1654.

(6) Dileptic refers to metal complexes containing only two types of ligands, e.g., $MnCp(CO)_3$.

(7) Lichtenberger, D. L.; Gruhn, N. E.; Rempe, M. E.; Geiger, W. E.; Chin, T. T. *Inorg. Chim. Acta* **1995**, *240*, 623.

10.1021/om800546d CCC: $40.75
Publication on Web 10/03/2008

donor solvents such as dichloromethane.[10] Among the studies most directly relevant to the present work are those involving $CoCp(CO)_2$[10c] and $Rh_2Fv(CO)_4$.[5]

An important factor that has emerged from the redox studies of fulvalendiyl complexes involves the *transoid* versus *cisoid* geometries of their redox pairs. Although the parent 36-electron compounds always have a *transoid* arrangement of the metal centers, removal of electrons may result in rearrangement into a *cisoid* structure in order to share electrons by forming a bond between the electron-deficient metal centers. This has been shown to occur for M_2FvL_2 when ML = $[Cr(CO)_3]^-$, $[Mo(CO)_3]^-$, $[Fe(CO)_2]^-$, $Rh(CO)(PPh_3)$, and $Rh(CO)_2$,[2,4,5] but, presumably owing to steric constraints, not with ML = $Mn(CO)_2PPh_3$.[3] The possibility of redox-promoted *transoid*/*cisoid* rotation is particularly relevant to the oxidation of **1**, as the dication $\mathbf{1}^{2+}$ would likely have 34 e^- diradical character without a structural rearrangement.[7] The present work is consistent with the structures of both the one-electron and two-electron oxidation products, $\mathbf{1}^+$ and $\mathbf{1}^{2+}$, respectively, adopting the *cisoid* structure in order to allow for Co−Co bond formation.

The accessibility of the oxidized forms of **1** raised the possibility of electron-transfer-induced metal−carbonyl substitution reactions, and such a process was observed in the presence of added PPh_3.

Experimental Section

A full description of the experimental procedures used in this work is available in a previous paper.[10c] The salient features are as follows.

All experiments were performed under nitrogen using either standard Schlenk conditions or a Vacuum Atmospheres drybox. Reagent-grade solvents were dried and vacuum distilled. Electrochemical glassware was oven-dried and placed in the drybox antechamber just prior to the experiment. $Co_2Fv(CO)_4$, **1**, had been prepared earlier by T. T. Chin based on a literature procedure.[11] It was purified by vacuum sublimation and checked for purity by NMR, IR, and C,H analysis. Electrochemical experiments were carried out in the drybox using a standard three-electrode configuration and a PARC 273A potentiostat interfaced to a personal computer. The glassy carbon working electrodes [disks of either 1.5 mm diameter (Cypress) or 1 or 2 mm diameter (Bioanalytical Systems)] were pretreated using a standard sequence of polishing with Buehler diamond paste, followed by washings with nanopure water, and final vacuum drying. The working electrode for bulk electrolyses was a basket-shaped platinum gauze.

All potentials given in this paper are referred to the ferrocene/ferrocenium reference couple.[12] When decamethylferrocene was used as an internal standard, the experimentally measured potential was converted to the ferrocene potential by addition of −0.61 V, which is the $E_{1/2}$ of decamethylferrocene vs $FeCp_2^{0/+}$ measured in CH_2Cl_2/0.05 M $[NBu_4][B(C_6F_5)_4]$ in our laboratory. Mechanistic aspects of redox processes were obtained from cyclic voltammetry (CV) data. Diagnostic criteria involving shapes and scan rate responses of the CV curves were applied using procedures described elsewhere.[13] Digital simulations were performed using Digisim 3.0 (Bioanalytical Systems). $[NBu_4][B(C_6F_5)_4]$ was prepared by metathesis of $[NBu_4]Br$ with $K[B(C_6F_5)_4]$ (Boulder Scientific, Boulder, CO) and purified as detailed elsewhere.[14] IR spectra were recorded with an ATI-Mattson Infinity Series FTIR instrument interfaced to a computer employing Winfirst software at a resolution of 4 cm^{-1}. NMR spectra were recorded using a Bruker ARX 500 MHz spectrometer, and ESR spectra were obtained on a Bruker ESP 300E spectrometer. IR spectroelectrochemistry was performed using a mid-IR fiber-optic "dip" probe (Remspec, Inc.), as described earlier.[15]

Results and Discussion

Electrochemistry of $Co_2Fv(CO)_4$, 1. The anodic oxidation of **1** in dichloromethane is strongly affected by the nature of the supporting electrolyte anion. Use of a traditional anion such as $[PF_6]^-$ results in strong adsorption problems, very likely due to the rapid precipitation of the hexafluorophosphate salt $[\mathbf{1}][PF_6]$ on the electrode surface.[16] Figure 1a gives an example of this behavior, which is reminiscent of that observed in the oxidation of $CoCp(CO)_2$ (Cp = η^5-C_5H_5).[10c] In contrast, essentially ideal diffusion-controlled behavior was observed with $[B(C_6F_5)_4]^-$ (TFAB) as the electrolyte anion. In CH_2Cl_2/0.05 M $[NBu_4][B(C_6F_5)_4]$, two well-separated and chemically reversible oxidations were observed (see Figure 1b) with $E_{1/2}(1)$ = 0.06 V and $E_{1/2}(2)$ = 0.51 V vs ferrocene$^{0/+}$. Peak separations ($E_{pa} - E_{pc}$) were 72−76 mV at slow CV scan rates, experimentally identical to the values observed for ferrocene under the same conditions. The chemical reversibility of both couples was established by attention to the diagnostic criteria of cyclic voltammetry (CV, scan rates 0.1 to 1 V s^{-1})[13] and double potential step chronoamperometry[17] (step time 1 s; $i_r(2\tau)/i_f(\tau) = 0.26$ for $\mathbf{1}/\mathbf{1}^+$, 0.25 for $\mathbf{1}/\mathbf{1}^{2+}$, 0.27 for ferrocene$^{0/+}$).

(8) (a) Basolo, F. *New J. Chem.* **1994**, *18*, 19. (b) Ruiz, J.; Lacoste, M.; Astruc, D. *J. Am. Chem. Soc.* **1990**, *112*, 5471. (c) Mao, F.; Tyler, D. R.; Keszler, D. *J. Am. Chem. Soc.* **1989**, *111*, 130. (d) Therien, M. J.; Trogler, W. C. *J. Am. Chem. Soc.* **1988**, *110*, 4942. (e) Therien, M. J.; Ni, C-L.; Anson, F. C.; Osteryoung, J. G.; Trogler, W. C. *J. Am. Chem. Soc.* **1986**, *108*, 4037. (f) Kochi, J. K. *J. Organomet. Chem.* **1986**, *300*, 139. (g) Downard, A. J.; Robinson, B. H.; Simpson, J. *Organometallics* **1986**, *5*, 1122. (h) Shi, Q-Z.; Richmond, T. G.; Trogler, W. C.; Basolo, F. *J. Am. Chem. Soc.* **1984**, *106*, 71. (i) Zizelman, P. M.; Amatore, C.; Kochi, J. K. *J. Am. Chem. Soc.* **1984**, *106*, 3771. (j) Hershberger, J. W.; Klingler, R. J.; Kochi, J. K. *J. Am. Chem. Soc.* **1983**, *105*, 61. (k) Hershberger, J. W.; Kochi, J. K. *J. Chem. Soc., Chem Commun.* **1982**, 212. (l) Hershberger, J. W.; Klingler, R. J.; Kochi, J. K. *J. Am. Chem. Soc.* **1982**, *104*, 3034. (m) Bruce, M. I.; Kehoe, D. C.; Matisons, J. G.; Nicholson, B. K.; Rieger, P. H.; Williams, M. L. *J. Chem. Soc., Chem. Commun.* **1982**, 442. (n) Bezems, G. J.; Rieger, P. H.; Visco, S. *J. Chem. Soc., Chem. Commun.* **1981**, 265.

(9) (a) Strauss, S. H. *Chem. Rev.* **1993**, *93*, 927. (b) Reed, C. A. *Acc. Chem. Res.* **1998**, *31*, 133. (c) Krossing, I.; Raabe, *Angew. Chem., Int. Ed.* **2004**, *43*, 2006.

(10) (a) Laws, D. R.; Chong, D; Nash, K; Rheingold, A. L.; Geiger, W. E. *J. Am. Chem. Soc.* **2008**, 130. (b) Chong, D.; Laws, D. R.; Nafady, A.; Costa, P. J.; Rheingold, A. L.; Calhorda, M. J.; Geiger, W. E. *J. Am. Chem. Soc.* **2008**, *130*, 2692. (c) Nafady, A.; Costa, P. J.; Calhorda, M. J.; Geiger, W. E. *J. Am. Chem. Soc.* **2006**, *128*, 16587. (d) Barriére, F.; Kirss, R. U.; Geiger, W. E. *Organometallics* **2005**, *24*, 48. (e) Chong, D.; Nafady, A.; Costa, P. J.; Calhorda, M. J.; Geiger, W. E. *J. Am. Chem. Soc.* **2005**, *127*, 15676. (f) Trupia, S.; Nafady, A.; Geiger, W. E. *Inorg. Chem.* **2003**, *42*, 5480. (g) Camire, N.; Nafady, A.; Geiger, W. E. *J. Am. Chem. Soc.* **2002**, *124*, 7260. (h) Camire, N; Mueller-Westerhoff, U. T.; Geiger, W. E. *J. Organomet. Chem.* **2001**, *637*−*639*, 823. (i) LeSuer, R. J.; Geiger, W. E. *Angew. Chem., Int. Ed.* **2000**, *39*, 248. (j) Hill, M. G.; Lamanna, W. M.; Mann, K. R. *Inorg. Chem.* **1991**, *30*, 4687.

(11) (a) Rausch, M. D.; Spink, W. C.; Conway, B. G.; Rogers, R. D.; Atwood, J. L. *J. Organomet. Chem.* **1990**, *383*, 227. (b) Vollhardt, K. P. C.; Weidman, T. W. *Organometallics* **1984**, *3*, 82.

(12) (a) Gritzner, G.; Kuta, J. *Pure Appl. Chem.* **1984**, *56*, 461. (b) Connelly, N. G.; Geiger, W. E. *Chem. Rev.* **1996**, *96*, 877.

(13) Geiger, W. E. In *Laboratory Techniques in Electroanalytical Chemistry*, 2nd ed.; Kissinger, P. T., Heineman, W. R., Eds.; Marcel Dekker: New York, 1996; Chapter 23.

(14) LeSuer, R. J.; Buttolph, C.; Geiger, W. E. *Anal. Chem.* **2004**, *76*, 6395.

(15) (a) Stoll, M. E.; Geiger, W. E. *Organometallics* **2004**, *23*, 5818. (b) Shaw, M. J.; Geiger, W. E. *Organometallics* **1996**, *15*, 13.

(16) The $[PF_6]^-$ anion does not appear to act as a nucleophile toward oxidized forms of **1**. $[Co_2Fv(CO)_4][PF_6]_2$ was isolated by performing a bulk electrolysis of **1** in CH_2Cl_2/0.05 M $[NBu_4][B(C_6F_5)_4]$ at 273 K, E_{appl} = 0.85 V, to generate $\mathbf{1}^{2+}$, followed by addition of $[NBu_4][PF_6]$, which provided a purple solid having the appropriate IR spectrum in Nujol (2147, 2121, 2100 (sh) cm^{-1}) and elemental analysis [C, 24.94 (25.72 calc); H, 1.23 (1.53 calc)].

(17) Bard, A. J.; Faulkner, L. R. *Electrochemical Methods*, 2nd ed.; John Wiley & Sons: New York, pp 207−210.

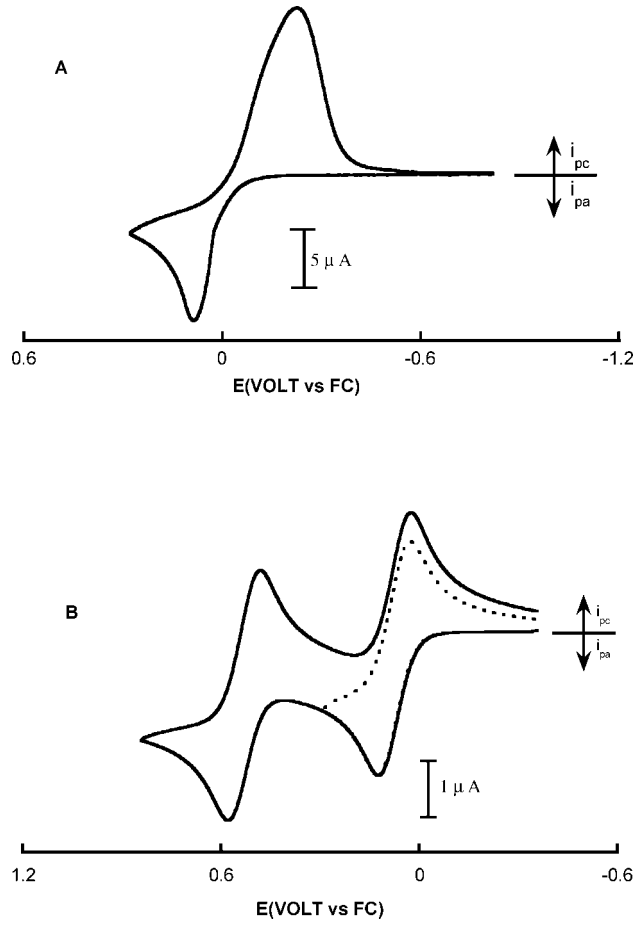

Figure 1. (A) Cyclic voltammogram of 1.2 mM **1** in CH_2Cl_2/0.1 M $[NBu_4][PF_6]$ at a scan rate of 0.2 V/s, 298 K on a 1 mm GC disk. (B) Cyclic voltammogram of 0.78 mM **1** in CH_2Cl_2/0.05 M $[NBu_4][B(C_6F_5)_4]$ at a scan rate of 0.1 V/s, 298 K on a 1 mm GC disk.

A diffusion coefficient of 1.54×10^{-5} cm^2 s^{-1} was determined for **1** from the chronoamperometry data.

Owing to the fact that the $[PF_6]^-$ salt of $\mathbf{1}^+$ adsorbs so strongly, the possible adsorption of $[\mathbf{1}][B(C_6F_5)_4]$ was probed by analysis[18] of chronocoulometric data obtained from the aforementioned double potential step experiments. Anson plots[19] constructed from this data (Figure 2) clearly demonstrate the lack of adsorption for the species **1**, $\mathbf{1}^+$, and $\mathbf{1}^{2+}$, confirming strictly diffusion-controlled behavior for both redox couples when TFAB is the electrolyte anion.

Square-wave voltammetry gave two well-shaped peaks wherein the height of the first wave became somewhat smaller than that of the second as the frequency was increased from 5 to 100 Hz (Figure 3), a qualitative indication that the first one-electron transfer is slightly slower than the second.[20] The entire collection of voltammetric data indicated that $Co_2Fv(CO)_4$ is oxidized in two well-separated one-electron steps according to eq 1, and the CV scans were successfully simulated (Figure 4).

$$Co_2Fv(CO)_4 \overset{-e^-}{\rightleftharpoons} [Co_2Fv(CO)_4]^+ \overset{-e^-}{\rightleftharpoons} [Co_2Fv(CO)_4]^{2+} \quad (1)$$

Bulk electrolysis experiments showed that the oxidized species were persistent over a longer time scale, even at ambient temperatures. Oxidation of an orange 0.55 mM solution of **1** at $E_{appl} = 0.85$ V gave a deep red solution of the dication $\mathbf{1}^{2+}$ after passage of 2.0 F. Linear scan voltammetry showed that the compound had converted quantitatively to the dication, and cathodic re-electrolysis at $E_{appl} = -0.2$ V regenerated neutral **1** in about 90% yield. Anodic oxidation at $E_{appl} = 0.35$ V provided a stable solution of the red monocation $\mathbf{1}^+$ as 1.02 F was passed. The oxidation of **1** was briefly investigated in other nonaqueous solvents. Two reversible one-electron oxidations were also observed in 1,2-dichloroethane and benzotrifluoride (BTF), with potentials as given in Table 1. Bulk coulometry in BTF confirmed the two one-electron processes, and about 70% of the starting material was obtained after its cyclic bulk

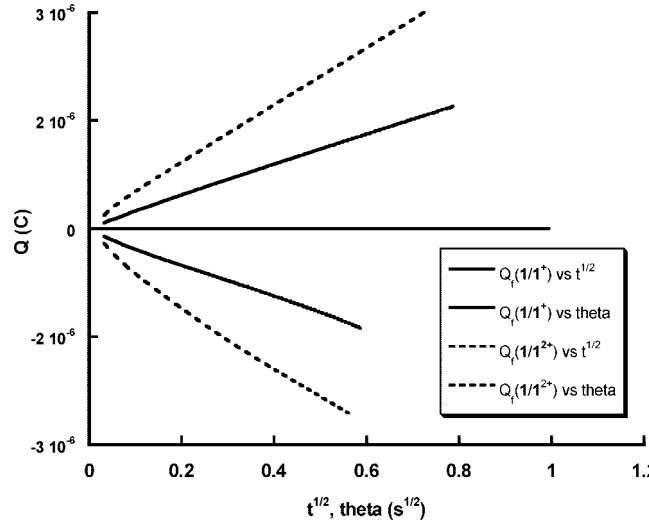

Figure 2. Anson plot for the two oxidation processes $\mathbf{1}/\mathbf{1}^+$ (solid lines) and the $\mathbf{1}/\mathbf{1}^{2+}$ (dotted lines) of 0.68 mM **1**, step time 1 s, 1 mm GC electrode.

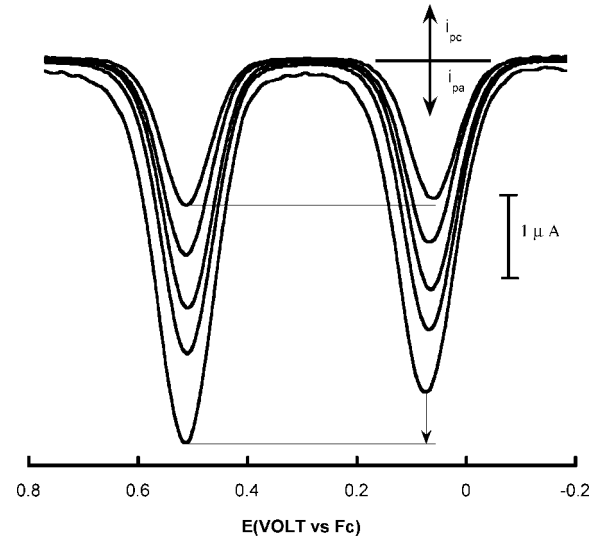

Figure 3. Different frequency square-wave voltammograms of 1 mM **1** in CH_2Cl_2/0.05 M $[NBu_4][B(C_6F_5)_4]$: increasing currents at frequencies of 5, 10, 25, 50, 100 Hz, 298 K, at 1 mm GC disk electrode.

(18) Reference 17, pp 210−214.

(19) (a) Anson, F. C.; Osteryoung, R. A. *J. Chem. Educ.* **1983**, *60*, 293. (b) Christie, J. J.; Anson, F. C.; Lauer, G.; Osteryoung, R. A. *Anal. Chem.* **1963**, *35*, 1979.

(20) Osteryoung, J.; O'Dea, J. J. In *Electroanalytical Chemistry*; Bard, A. J., Ed.; Marcel Dekker, Inc.: New York, 1986; Vol. 14, pp 231−237.

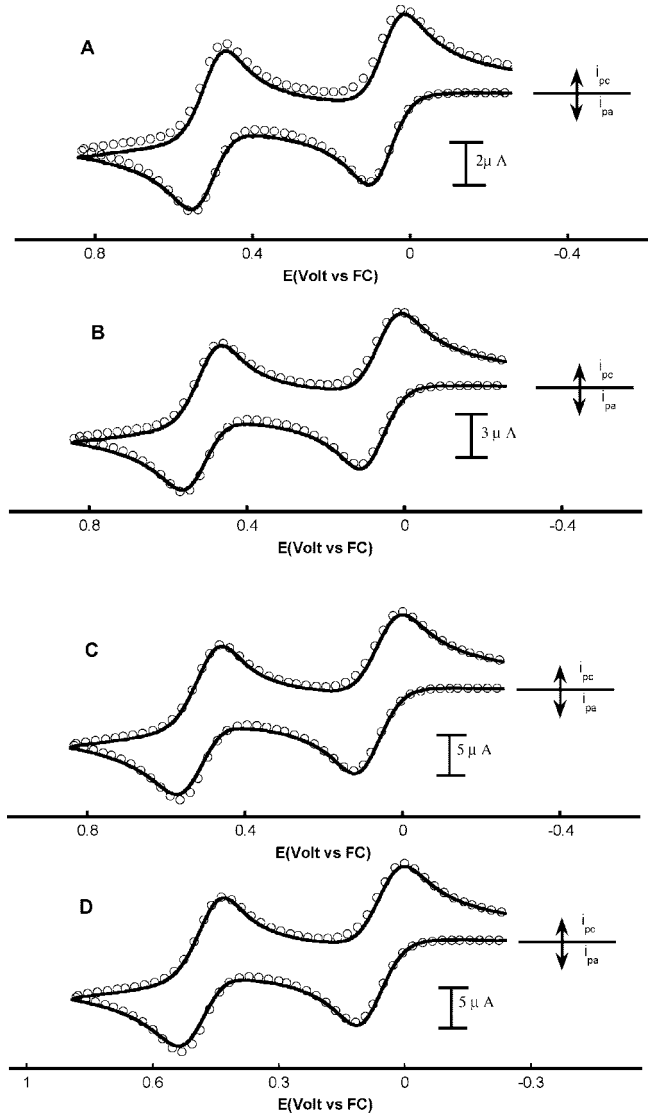

Figure 4. Experimental (solid lines) and simulated (circles) cyclic voltammograms of 1.25 mM **1** at scan rates (a) 0.1, (b) 0.2, (c) 0.5, (d) 1 V/s in CH_2Cl_2/0.05 M $[NBu_4][B(C_6F_5)_4]$ at 1 mm GC disk electrode, 298 K. See Table 3 for relevant simulation parameters.

Table 1. $E_{1/2}$ Potentials (volts vs ferrocene) of 1 in Different Solvents with 0.05 M $[NBu_4][TFAB]$ as Supporting Electrolyte, DCE = dichloroethane, BTF = benzotrifluoride

solvent	$E_{1/2}(1)$	$E_{1/2}(2)$	$\Delta E_{1/2}$ (mV)
CH_2Cl_2	0.06	0.51	450
DCE	0.05	0.50	450
BTF	0.06	0.53	470

oxidation and rereduction. The first oxidation of **1** was chemically irreversible in THF owing, no doubt, to the reaction of $\mathbf{1}^+$ with this donor solvent.

It is to be noted that the first oxidation potential of **1** is 310 mV negative of that reported for its mononuclear "parent" $CoCp(CO)_2$.[10c] Given that there is only a weak electronic interaction between the metal centers in the neutral complex,[7] facilitation of the oxidation most likely arises from the very rapid structural change that accompanies the loss of an electron from **1**.

Spectral Characterization of the Oxidation Products $\mathbf{1}^+$ and $\mathbf{1}^{2+}$. Infrared spectra were obtained either by syringe-removal of electrolysis samples or by *in situ* IR spectroelectrochemistry using a fiber-optic "dip" probe. The former, shown in Figure 5, was used to obtain the IR assignments given in Table 2. The two major carbonyl bands moved from 2020, 1962 cm^{-1} in **1** to 2147, 2122 cm^{-1} in $\mathbf{1}^{2+}$, an average increase of 143.5 cm^{-1}. For comparison, an average shift of 126 cm^{-1} was observed for ν_{CO} in the oxidation of $CoCp(CO)_2$ to the metal−metal bonded dimer $[Co_2Cp_2(CO)_4]^{2+}$.[10c] The most revealing aspect of the IR data was the presence of three intense carbonyl bands (2096, 2054, 2030 cm^{-1}) in the spectrum of $\mathbf{1}^+$, caused by strong vibrational coupling, which is indicative

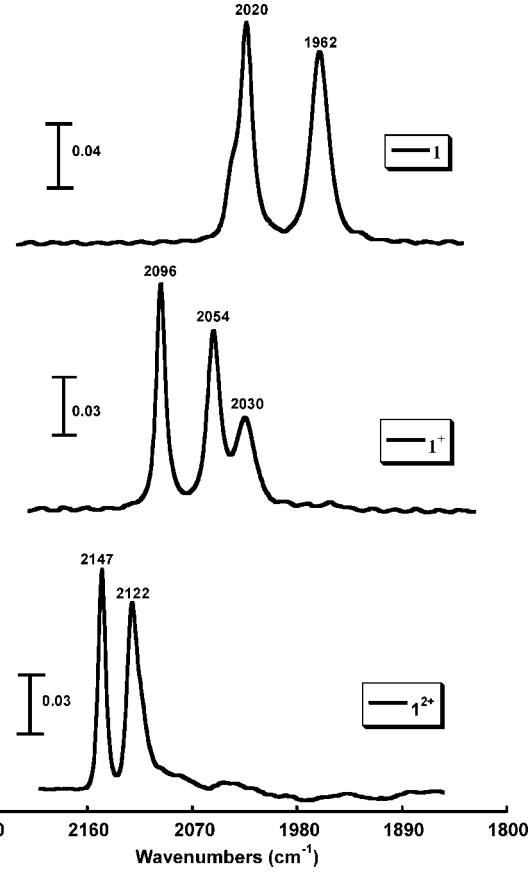

Figure 5. IR spectra of a solution of 1.2 mM **1** in CH_2Cl_2/0.05 M $[NBu_4][B(C_6F_5)_4]$ before and after electrolysis at the first and second oxidation waves at 298 K.

Table 2. Carbonyl-Region IR Energies for Different Redox States of $Co_2Fv(CO)_4$ (1) and $Co_2Fv(CO)_3(PPh_3)$ in CH_2Cl_2

cmpd or ion	ν_{CO} (cm^{-1})	av shift[a] (cm^{-1})	shift[a] (cm^{-1})
1	2020 (vs),[b] 1962 (vs)	n.a.	n.a.
$\mathbf{1}^+$	2096 (vs), 2054 (vs), 2030 (s)	69	76
$\mathbf{1}^{2+}$	2147 (vs), 2122 (vs)	143.5	127
2	2020 (vs), 1958 (vs), 1925 (w)	n.a.	n.a.
$\mathbf{2}^+$	2049 (vs), 2032 (s), 1976	51	29
$\mathbf{2}^{2+}$	2114 (vs), 2091(s), 2063(w)	138	96

[a] Largest shift = difference between highest energy ν_{CO} band of oxidized compound and neutral compound; av shift = average difference between energies of two or three resolved ν_{CO} bands in the oxidized and neutral compounds. [b] Relative intensity designations: vs = very strong, s = strong, w = weak.

Table 3. Thermodynamic and Kinetic Parameters Used for Digital Simulation for Compounds 1 and 2 via the Mechanism Shown in Scheme 1

cmpd	E^0_1 (V)	k_s^1 (cm/s)	E^0_2 (V)	k_s^2 (cm/s)	k_f^1 (M^{-1} s^{-1})	K_{eq}^1 (M^{-1})
1	0.06	0.015	0.51	0.02	5×10^3	1×10^5
2	−0.36	0.025	0.19	0.01	n.a	n.a

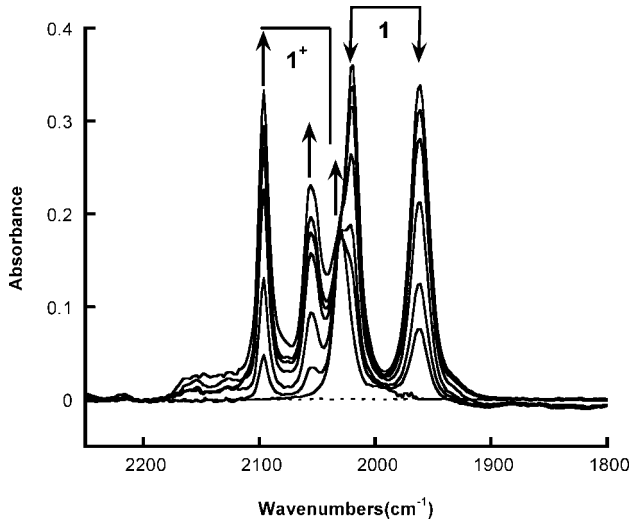

Figure 6. *In situ* IR spectroelectrochemistry of 1 mM **1** in CH_2Cl_2 /0.05 $[NBu_4][B(C_6F_5)_4]$ recorded during bulk electrolysis at the first oxidation wave of **1** at 298 K.

of a *direct link* between cobalt atoms. IR spectra therefore are consistent with a *cisoid* structure of $\mathbf{1}^+$ accompanied by formation of a metal−metal bond. Using simple average values, the ν_{CO} energies increase by 69 cm^{-1} on going from **1** to $\mathbf{1}^+$, again in concert with the effect of a one-half increase in positive charge at the $Co(CO)_2$ moieties (an increase of 75 cm^{-1} was reported on going from $CoCp(CO)_2$ to $[Co_2Cp_2(CO)_4]^+$)[10c]. Confirmation of the spectral assignment of $\mathbf{1}^+$ was obtained in an *in situ* IR experiment, in which an isosbestic point was observed for the conversion of **1** to $\mathbf{1}^+$ (Figure 6).

ESR spectra of $\mathbf{1}^+$ were obtained in both fluid and frozen solutions (Figure 7). The former ($\langle g \rangle = 2.072$) displays hyperfine splittings (hfs) consistent with interaction of two equivalent ^{59}Co nuclei ($I = 7/2$), 13 of the expected 15 lines being resolved, $\langle A \rangle = 10$ G. The glassy spectrum also was consistent with two equivalent Co hfs having a major value, $A(1)$, of 47 G, but its complexity allowed only a partial analysis. If it is assumed that the radical has axial symmetry and that $\langle A \rangle$ and $A(1)$ have the same sign, a value of −8.5 G is calculated for $A(2)$ and $A(3)$, based on the fact that $\langle A \rangle = 1/3(A(1) + A(2) + A(3))$. This allows an estimate to be made of the spin density on cobalt, using eqs 2 and 3 for an axial hfs pattern.[21]

$$A_{\parallel} = \langle A \rangle + 2B \quad (2)$$

$$A_{\perp} = \langle A \rangle - B \quad (3)$$

In this treatment, the uniaxial hyperfine constant, B, is calculated to be 19 G (1.9 mT). Since the theoretical B value for 100% spin on cobalt is 12.1 mT,[21] the *combined* spin density on the two metals is calculated to be about 1/3 of an electron. This number may be a bit low, given the assumptions made in our analysis, but it seems safe to conclude that a significant amount of spin density in $\mathbf{1}^+$ is delocalized into the CO ligands and the fulvalendiyl π system.

The ESR spectra are much different from those observed for the *transoid* radical cation $[Co_2Fv(COD)_2]^+$, COD = 1,5-cyclooctadiene, reported earlier by Chin[22] and given a more detailed analysis based on the work of Rieger et al.[23] on the

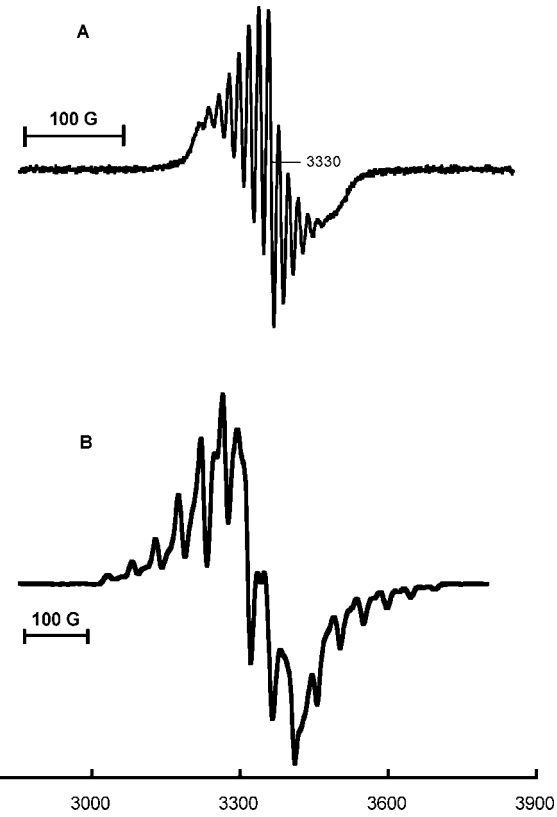

Figure 7. (A) ESR fluid spectra of $\mathbf{1}^+$ in CH_2Cl_2/0.05 M $[NBu_4][B(C_6F_5)_4]$, generated by bulk oxidation at the potential of the first wave of 0.55 mM **1** at 298 K. (B) ESR frozen spectra recorded at 140 K of ca. 1 mM $\mathbf{1}^+$ produced under similar conditions.

mononuclear system $[CoCp(COD)]^+$. The spread in g values for $[Co_2Fv(COD)_2]^+$ was quite large (>0.3) compared to the small spread for $\mathbf{1}^+$, with the largest Co hfs splitting being found in the lowest-field g component, rather than the highest, as seen for $\mathbf{1}^+$. The class II mixed-valence structure of $[Co_2Fv(COD)_2]^+$, in which about 2/3 of the spin density is located on a *single* Co,[22] contrasts starkly with the shared electron density of the metals in $\mathbf{1}^+$.

Another well-studied system that is relevant to the findings for $\mathbf{1}^+$ is the anion radical $[Co_2Cp_2(\mu\text{-}CO)_2]^-$, reported by Schore et al.[24] Although there are clear structural differences between these two systems, with $[Co_2Cp_2(\mu\text{-}CO)_2]^-$ having bridging carbonyls and a bond order of 1.5 between the metals, each possesses a formally 18 e^-/17 e^- pair of metals. The ESR spectra of $[Co_2Cp_2(\mu\text{-}CO)_2]^-$ have been analyzed both by Schore[24a] and by Symons and Bratt.[25] Compared to $\mathbf{1}^+$, the isotropic hfs value $\langle A \rangle$ was considerably larger (ca. 50 vs 10 G for $\mathbf{1}^+$), as was the largest anisotropic Co hfs (ca. 90 vs 47 G for $\mathbf{1}^+$). Owing, however, to the fact that $\langle A \rangle$ is considerably larger than $A(2)$ or $A(3)$, analysis using eqs 2 and 3 gives a B value (20 G) that is very similar to that determined for $\mathbf{1}^+$, implying similar Co d orbital contributions in the two systems.

(21) Weil, J. A.; Bolton, J. R.; Wertz, J. E. *Electron Paramagnetic Resonance*; John Wiley & Sons: New York, 1994; p 116. For the uniaxial hyperfine constant of Co, see p 534

(22) Chin, T. T.; Geiger, W. E. *Organometallics* **1995**, *14*, 1316.

(23) Rieger, P. H.; Chin, T. T.; Sharp, L. I.; Geiger, W. E. *Organometallics* **1995**, *14*, 1322.

(24) (a) Schore, N. E. *J. Organomet. Chem.* **1979**, *173*, 30. (b) Schore, N. E.; Ilenda, C. S.; Bergman, R. G. *J. Am. Chem. Soc.* **1977**, *99*, 1781. (c) Ilenda, C. S.; Schore, N. E.; Bergman, R. G. *J. Am. Chem. Soc.* **1976**, *98*, 255. (d) Schore, N. E.; Ilenda, C. S.; Bergman, R. G. *J. Am. Chem. Soc.* **1976**, *98*, 256.

(25) Symons, M. C. R.; Bratt, S. W. *J. Chem. Soc., Dalton Trans.* **1979**, 1739.

Using somewhat different analyses and values for the theoretical uniaxial hyperfine constant, Schore gave a higher estimate of the degree of metal character in $[Co_2Cp_2(\mu\text{-}CO)_2]^-$, ca. 60%. Although clarity in interpreting the ESR spectra of $\mathbf{1}^+$ would profit from better resolved spectra, it is reasonable to conclude that the SOMO of $\mathbf{1}^+$ contains considerable contributions from both metal and ligand orbitals. This conclusion might appear to be inconsistent with the calculations of Lichtenberger et al., who found a HOMO localized in a *single* Co d_{yz} orbital for **1**,[7] but the significant structural change that accompanies charge transfer (i.e., *transoid* **1** to *cisoid* $\mathbf{1}^+$) explains the change in electronic structure.

Absorption spectra in the UV to NIR range (300 to 2000 nm) were also measured for the present dicobalt system. The lowest energy absorption for $\mathbf{1}^+$ was an intense band at 712 nm ($\varepsilon = 3.9 \times 10^3$ M^{-1} cm^{-1}). The dication $\mathbf{1}^{2+}$ had an intense transition at 360 nm ($\varepsilon = 1.0 \times 10^4$ M^{-1} cm^{-1}) as well as a band at $\lambda_{max} \approx 520$ nm ($\varepsilon = 3.1 \times 10^3$ M^{-1} cm^{-1}) that appeared to be overlapped with another feature at slightly higher energy. Both metal σ/σ^* transitions[26] and ligand-to-metal charge-transfer transitions are expected for the cations derived from **1**. Spectra are available as Figure SM1 of the Supporting Information.

Substitution of CO by PPh_3 in $\mathbf{1}^+$. The thermally driven substitution of one or more carbonyl groups by phosphine ligands is known to be slow (e.g., 24 h reflux) for the mononuclear parent complex $CoCp(CO)_2$.[27] Given the well-known increase in the lability of carbonyls in 17-electron systems,[8] it seemed reasonable to investigate the possibility of anodically induced substitution reactions in the oxidation products of **1**.

When PPh_3 is added to solution, the changes observed in the CV of **1** are consistent with a substitution process taking place for the monocation $\mathbf{1}^+$. Decreases are observed in the chemical reversibility of the $\mathbf{1}/\mathbf{1}^+$ process and in the height of the second oxidation wave (due to less $\mathbf{1}^+$ available for further oxidation), and two new reversible redox waves appear. These alterations are shown in Figure 8 for the stepwise addition of up to 1 equiv of PPh_3, where the effects on **1** as well as the new features at $E_{1/2} = 0.19$ and -0.36 V may be followed by the vertical arrows. The relative heights of these four waves were independent of scan rate over the range from 0.1 to 1 V s^{-1} (Figure 9), indicating that the follow-up substitution reaction is fast on the voltammetric time scale.

When bulk electrolysis was carried out at a potential ($E_{appl} = 0.4$ V) sufficient to oxidize **1** to the *mono*cation $\mathbf{1}^+$, almost *two* faradays of charge were released (1.8 F at either room temperature or 273 K) as an olive-colored solution was formed. The major product waves were the new pair at 0.19 and -0.36 V, attributed to the two one-electron reactions of the monosubstitution product $Co_2Fv(CO)_3(PPh_3)$, **2**, eq 4:

$$\underset{\mathbf{2}}{Co_2Fv(CO)_3(PPh_3)} \underset{-0.36\ V}{\overset{-e^-}{\rightleftharpoons}} \underset{\mathbf{2}^+}{[Co_2Fv(CO)_3(PPh_3)]^+} \underset{0.19\ V}{\overset{-e^-}{\rightleftharpoons}} \underset{\mathbf{2}^{2+}}{[Co_2Fv(CO)_3(PPh_3)]^{2+}} \quad (4)$$

The potential assigned to $\mathbf{2}/\mathbf{2}^+$ (-0.36 V) is close to that reported[28] for the mononuclear analogue $CoCp(CO)(PPh_3)^{0/+}$ (-0.33 V when converted from SCE to ferrocene reference[12b]), confirming the monosubstitution process.

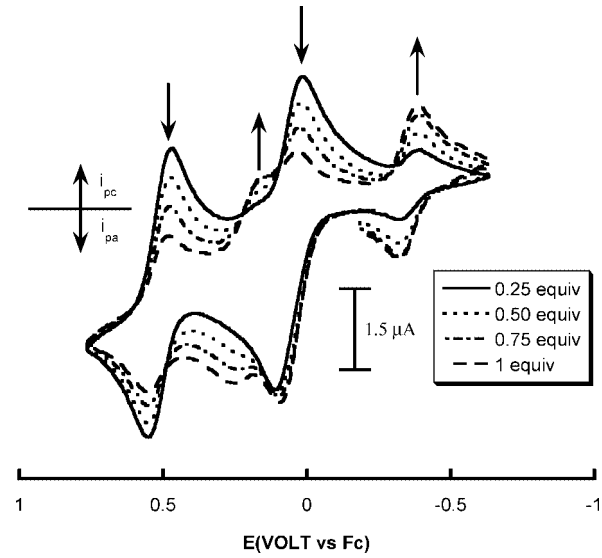

Figure 8. Cyclic voltammograms of 0.55 mM **1** in CH_2Cl_2/0.05 M $[NBu_4][B(C_6F_5)_4]$ at a scan rate of 500 mV/s after addition of 0.25, 0.5, 0.75, and 1 equiv of PPh_3.

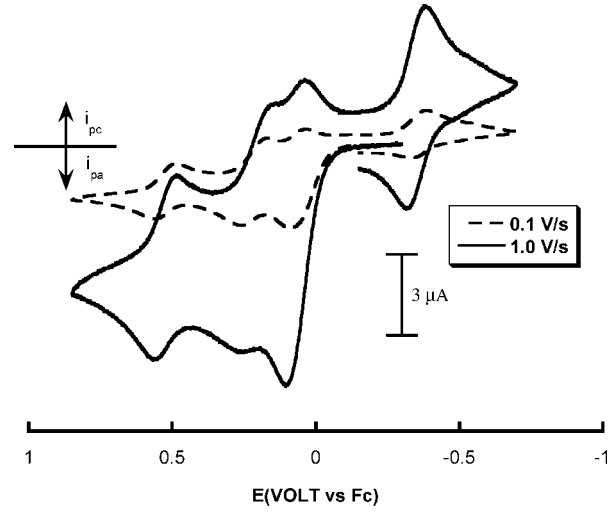

Figure 9. Cyclic voltammograms of 1 mM **1** with 1 equiv PPh_3 in CH_2Cl_2/0.05 M $[NBu_4][B(C_6F_5)_4]$ at different scan rates.

The net two-electron nature of the electrolysis at a potential *insufficient* to form the dication $\mathbf{1}^{2+}$ arises from the fact that when $\mathbf{2}^+$ is formed at $E_{appl} = 0.4$ V, the substitution product $\mathbf{2}^+$ is oxidized to the dication $\mathbf{2}^{2+}$, which is the final product under these conditions. As will be shown below, $\mathbf{2}^{2+}$ may be reduced sequentially, first to $\mathbf{2}^+$ and then to **2**, by carefully controlled cathodic "back-electrolysis" of the product. IR spectra of fully oxidized $\mathbf{2}^{2+}$ showed strong carbonyl bands at 2114, 2091, and 2063 cm^{-1} (Table 2), the first two of which are ascribed to the $\{Co(CO)_2\}^+$ moiety, the last being assigned to the $\{Co(CO)(PPh_3)\}^+$ moiety. Doing so establishes an average oxidative shift of 111.5 cm^{-1} for the $Co(CO)_2$ group, somewhat lower than the 143.5 cm^{-1} obtained for the same quantity when the tetracarbonyl compound **1** undergoes two-electron oxidation. The lower shift may be ascribed to the substituent effect (replacement of a CO by the more electron-donating PPh_3 group) on the adjacent metal center. When the dication $\mathbf{2}^{2+}$ is fully reduced back to **2**, the substituted neutral complex has three CO bands, at 2020, 1958, and 1925 cm^{-1}. Since the first two

(26) Abrahamson, H. B.; Palazzotto, M. C.; Reichel, C. L.; Wrighton, M. S. *J. Am. Chem. Soc.* **1979**, *101*, 4127.

(27) (a) Hart-Davis, A. J.; Graham, W. A. G. *Inorg. Chem.* **1970**, *9*, 2658. (b) Schuster-Wolden, H. G.; Basolo, F. *J. Am. Chem. Soc.* **1966**, *88*, 1657.

(28) Broadley, K.; Connelly, N. G.; Geiger, W. E. *J. Chem. Soc., Dalton Trans.* **1983**, 121.

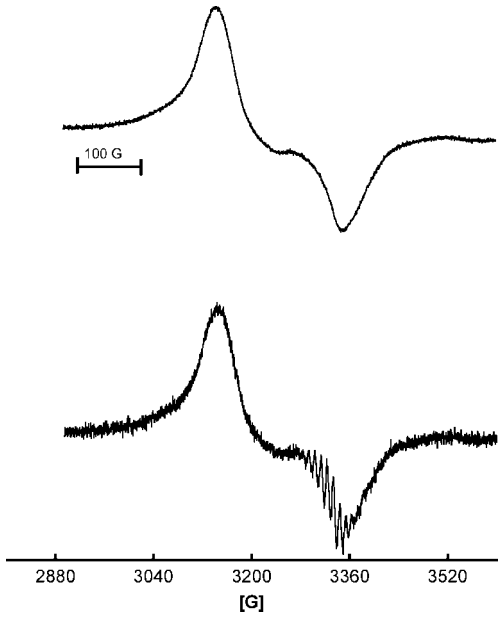

Figure 10. (Top) Fluid solution ESR spectrum of the 2^+ in CH_2Cl_2/0.05 M $[NBu_4][B(C_6F_5)_4]$, 298 K, microwave power = 20 mW, frequency = 9.448 GHz, modulation amplitude = 25 G. (Bottom) Fluid solution ESR spectrum of 2^+ under the same conditions at 298 K, microwave power = 40 mW, modulation amplitude = 5 G.

are essentially at the same frequencies as seen for the dicarbonyl groups in **1**, the 1925 cm^{-1} band is assigned to the carbonyl of the $Co(CO)(PPh_3)$ group. Thus an increase of 2063 − 1925 = 138 cm^{-1} is measured for the loss of one electron from the $Co(CO)(PPh_3)$ group, confirming the IR assignments for 2^{2+}.

This leaves only the assignment of IR frequencies in the monocation 2^+. Owing to the fact that the phosphine-containing metal center is easier to oxidize than the dicarbonyl-based metal, the positive charge of 2^+ is expected to lie largely on the Co-phosphine side of the radical cation. One-electron bulk reduction of 2^{2+} ($E_{appl} = -0.15$ V) to 2^+ gave new bands at 2049, 2032, and 1976 cm^{-1} in addition to some bands from the apparent partial regeneration of **1**. The 2049 cm^{-1} band is assigned to the $\{Co(CO)(PPh_3)\}^+$ moiety, shifted slightly from the 2063 cm^{-1} of 2^{2+} owing to linkage with the neutral $Co(CO)_2$ group. Bands assigned to the $\{Co(CO)_2\}$moiety in 2^+ (at 2032 and 1976 cm^{-1}) are shifted by an amount that is similar in size, but opposite in direction, from neutral $Co(CO)_2$ groups in both **1** and **2**. In this case, the shift to higher energy is rationalized by the linkage to the positively charged $\{Co(CO)(PPh_3)\}^+$ group.

The ESR spectrum of 2^+ in fluid solutions, while not definitive about the electronic structure of the radical, is also consistent with assignment of the positive charge to the $\{Co(CO)(PPh_3)\}$ moiety. A very broad signal lacking any resolved hyperfine splittings was observed (Figure 10) having $g = 2.084$, in concert with previous observations for $[CoCp^*(CO)(PPh_3)]^+$ ($Cp^* = C_5Me_5$) and $[CoCp(CO)(PCy_3)]^+$ (Cy = cyclohexyl).[28] Visual inspection of the spectrum (Figure 10, top) reveals some asymmetry on the high-field side that arises, in fact, from a superposition with the spectrum of a minor radical. At lower values of the magnetic field modulation amplitude, the sharper features of the second radical were revealed (Figure 10, bottom), allowing its assignment to 1^+ based on its g value and hyperfine splittings. Its presence may arise either from incomplete phosphine substitution or from partial loss of phosphine in the reverse electrolysis.

Scheme 1

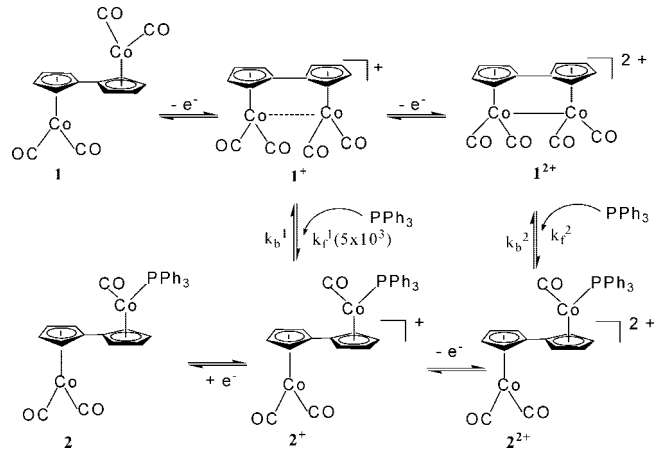

Having identified the primary substitution product as $[Co_2Fv(CO)_3(PPh_3)]^+$, digital simulations of CV curves were undertaken to confirm the overall process of Scheme 1.

Simulations were performed for background-subtracted CV scans from 0.2 to 1.0 V s^{-1} in which ohmic loss was partially compensated. Transfer coefficients were kept at $\alpha = 0.5$ and the diffusion coefficients were kept identical for differently charged species of the same compound, using the measured value of $D_o = 1.53 \times 10^{-5}$ cm^2 s^{-1} for **1** and an estimated value of $D_o = 1 \times 10^{-5}$ cm^2 s^{-1} for **2**. The parameters for the

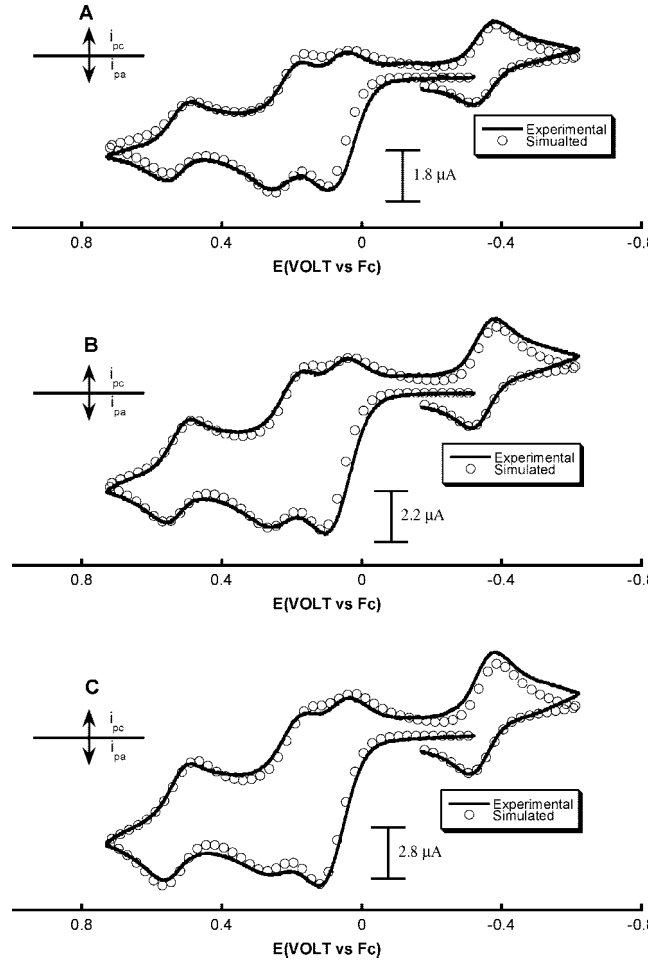

Figure 11. Experimental and simulated cyclic voltammograms of 1.1 mM **1** in CH_2Cl_2/0.05 M $[NBu_4][B(C_6F_5)_4]$ and 1 equiv of PPh_3 at different scan rates; A = 0.2, B = 0.5, C = 1 V/s.

Scheme 2

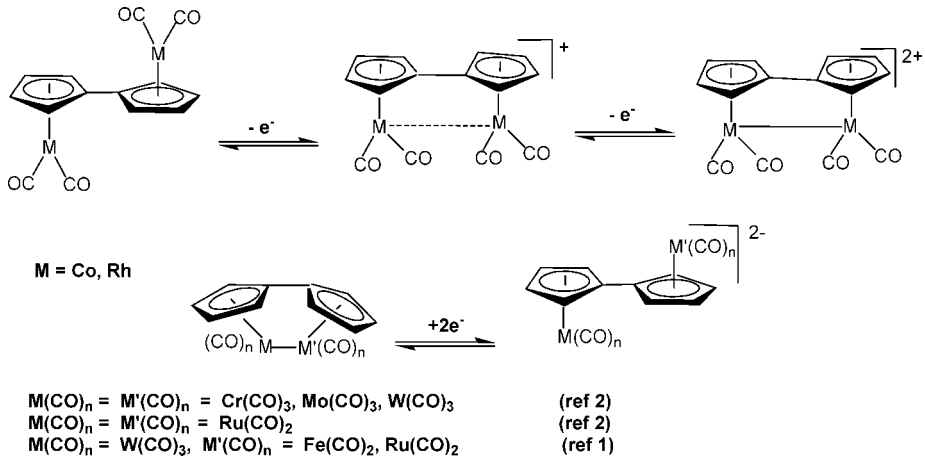

couples $\mathbf{1}/\mathbf{1}^+$ and $\mathbf{1}^+/\mathbf{1}^{2+}$ were those previously determined for the tetracarbonyl complex (*vide ante*). It is expected that, besides the reaction of $\mathbf{1}^+$ with PPh_3, a substitution process will also occur between PPh_3 and $\mathbf{1}^{2+}$ (eq 5).

$$[Co_2Fv(CO)_4]^{2+} + PPh_3 \rightleftharpoons [Co_2Fv(CO)_3(PPh_3)]^{2+} \quad (5)$$

Although this reaction was also considered in simulations, its inclusion improved the fits only slightly, allowing the qualitative conclusion that the rates and equilibrium constants for the substitution processes in $\mathbf{1}^+$ and $\mathbf{1}^{2+}$ appear to be roughly the same order of magnitude. As demonstrated in Figure 11, reasonable fits were obtained even when eq 5 was not included in the calculations. As summarized in Table 3, the values of both $K_{sub}{}^1$ ($= k_f{}^1/k_b{}^1$) and $k_f{}^1$ were shown to be large ($\geq 10^5$ M^{-1} and $\geq 5 \times 10^3$ M^{-1} s^{-1}, respectively), confirming that the substitution of CO by PPh_3 in the radical cation $\mathbf{1}^+$ is thermodynamically highly favored and kinetically rapid on the voltammetric time scale.

Conclusions

A number of attempts made in the past to study the anodic reactions of neutral dileptic fulvalenediyl compounds have been thwarted by the poor solubilities of the cationic electrode products, which caused strong electrode adsorption and, eventually, electrode passivation. These problems were not overcome even by carrying out the electrochemistry in polar solvents such as acetonitrile and propylene carbonate, which added another concern, namely, the possibility of nucleophilic attack on the oxidized species by a donor solvent.[1b,2a,3a] As shown in a recent paper,[5] both of these problems (adsorption and nucleophilic attack) are circumvented when performing the oxidation in a gentle medium made up of a nondonor solvent and a WCA-based electrolyte. Taking this approach, the fulvalenediyl compound $Co_2Fv(CO)_4$ was shown to be oxidized in two discrete one-electron steps to soluble cationic species that were sufficiently persistent to be characterized *in situ* by IR, UV−vis, and ESR techniques. The $E_{1/2}$ separation of the two one-electron processes $\mathbf{1}/\mathbf{1}^+$ and $\mathbf{1}^+/\mathbf{1}^{2+}$ in CH_2Cl_2/0.05 M $[NBu_4][TFAB]$ was 450 mV, significantly greater than the value of 80 mV observed for the dirhodium congener.[5] However, as with $[Rh_2Fv(CO)_4]^+$, metal−metal bond formation is evident from the ESR and IR spectra of $[Co_2Fv(CO)_4]^+$, demonstrating that a *transoid* to *cisoid* structural change accompanies the one-electron oxidation of **1**. No cationic *transoid* or neutral *cisoid* intermediates were observed voltammetrically for these systems, making it possible that the *transoid/cisoid* structure changes (see Scheme 2, group 9) are concerted with electron transfer, but a more complex square-scheme mechanism cannot be ruled out.[29] The overall preference for a metal−metal bonded structure in the electron-deficient oxidation products is consistent for group 6, group 8, and group 9 metals. However, the one-electron redox intermediate may be observed for the group 9 fulvalenediyl complexes, in contrast to the single two-electron reactions observed for complexes of the other metal groups.[1,2] These quite different behaviors are not likely to arise from electrolyte effects, since the group 6 and group 8 redox processes do not involve positively charged products. Hence, it is likely that the direct two-electron processes of the Cr and Fe groups can be traced to stronger M−M bonds, which preferentially stabilize the twice-oxidized complexes, consistent with the model proposed in previous literature.[1,2] The group 9 systems would, by inference, possess weaker M−M bonds.

The kinetic stability of the oxidized products of **1** in TFAB-containing media make possible the facile substitution of a single carbonyl group by PPh_3, allowing for the electrochemical and spectral characterization of the phosphino derivative $[Co_2Fv(CO)_3(PPh_3)]^{n+}$ in three different redox states ($n = 0, 1, 2$).

Acknowledgment. We gratefully acknowledge support by NSF (CHE-0411703) and thank Boulder Scientific Co. for a partial donation of electrolyte anions.

Supporting Information Available: Visible/near-IR spectra of **1**, $\mathbf{1}^+$, and $\mathbf{1}^{2+}$. This material is available free of charge via the Internet at http://pubs.acs.org.

OM800546D

(29) The difficulty in delineating between fast square schemes and concerted electron-transfer/structural change mechanisms has been recently discussed in: Geiger, W. E. *Organometallics* **2007**, *26*, 5738.